JOC Article

Mechanism of the Gold-Catalyzed Rearrangement of (3-Acyloxyprop-1-ynyl)oxiranes: A Dual Role of the Catalyst

Adán González Pérez,[†] Carlos Silva López,[†] José Marco-Contelles,[‡] Olalla Nieto Faza,*[,†] Elena Soriano,*[,‡] and Angel R. de Lera*[,†]

Departamento de Química Orgánica, Facultade de Química, Universidade de Vigo, 36310 As Lagoas-Marcosende s/n, Spain, and Laboratorio de Radicales Libres, Instituto de Química Orgánica General, CSIC, 28006 Madrid, Spain

faza@uvigo.es; esoriano@iqog.csic.es; qolera@uvigo.es

Received November 11, 2008

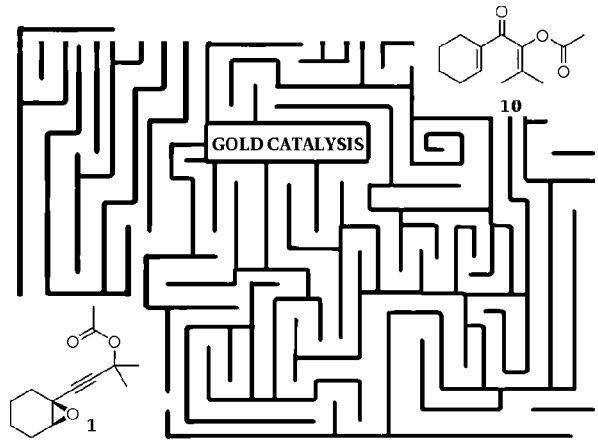

The three competing paths for the rearrangement of **1** (involving 1,2- and 1,3-ester migration with alkyne or oxirane activation) evidence the multifaceted character of gold as a catalyst. The most favorable mechanism for this useful synthetic transformation involves a cascade of more than eight steps. All the functional groups in the substrate play a crucial and synergistic role, and sequential gold coordination to both the π-system and the lone pairs of oxygen is needed. Exploration of these three paths suggests the use of a nonalkynophilic Lewis acid (BF_3) as a possible synthetic alternative for this transformation.

Introduction

The use of gold(I) and gold(III) complexes as efficient homogeneous catalysts in a wide variety of organic transformations has been highlighted in the last years.[1] The popularity of these processes, which allow the formation of both C−C and C−X bonds, is largely due to the significant increase in molecular complexity and the impressive structural diversity they can provide.[2] In many of these processes, the alkynophilic character of gold complexes and the π-acid activation of unsaturated precursors promote the attack of a nucleophilic entity, thus providing an atom-economical entry into cyclic and acyclic scaffolds useful for the synthesis of a wide range of products. As a result, alkynes have emerged as excellent, highly versatile precursors able to react selectively at the two unsaturated carbon positions. Upon coordination, gold catalysts activate the triple bond toward nucleophilic addition, yielding carbenoid intermediates which generate different cyclic adducts depending on the molecular structure.[3]

[†] Universidade de Vigo.
[‡] Instituto de Química Orgánica General, CSIC.

(1) (a) Gorin, D. J.; Toste, F. D. *Nature* **2007**, *446*, 395. (b) Chianese, A. R.; Lee, S. J.; Gagné, M. R. *Angew. Chem., Int. Ed.* **2007**, *46*, 4042. (c) Ma, S.; Yu, S.; Gu, Z. *Angew. Chem., Int. Ed.* **2006**, *45*, 200. (d) Bruneau, C. *Angew. Chem., Int. Ed.* **2005**, *44*, 2328.

(2) (a) Li, Z.; Brouwer, C.; He, C. *Chem. Rev.* **2008**, *108*, 3239. (b) Jiménez-Núñez, E.; Echavarren, A. M. *Chem. Rev.* **2008**, *108*, 3326. (c) Bongers, N.; Krause, N. *Angew. Chem., Int. Ed.* **2008**, *47*, 2178. (d) Fürstner, A.; Davies, P. W. *Angew. Chem., Int. Ed.* **2007**, *46*, 3410. (e) Zhang, L.; Sun, J.; Kozmin, S. A. *Adv. Synth. Catal.* **2006**, *348*, 2271. (f) Hashmi, A. S. K.; Hutchings, G. J. *Angew. Chem., Int. Ed.* **2006**, *45*, 7896.

(3) Some studies suggest that these intermediates might be better described as cationic species: (a) Fürstner, A.; Szillat, H.; Gabor, B.; Mynott, R. *J. Am. Chem. Soc.* **1998**, *120*, 8305. (b) Hashmi, A. S. K. *Angew. Chem., Int. Ed.* **2008**, *47*, 6754.

10.1021/jo802516k CCC: $40.75
Published on Web 03/26/2009

Propargylic esters[4] are particularly useful in this kind of transformations, since the migratory ability of the carboxylic group to any of the two unsaturated positions can lead to a diverse and rich reactivity.[5] In these systems, the ester may compete with other nucleophiles and perform an internal 1,2- or 1,3-rearrangement upon electrophilic activation of the alkyne.[6] The former process affords gold vinyl carbenoids, which can be trapped by a nucleophile,[7,8] while the latter generates allenic structures, which are further activated by a gold catalyst for subsequent reactivity.[9] Despite other factors coming into play, the 1,2-ester migration is favored for terminal whereas the 1,3-rearrangement becomes a competing, or even the leading, path for internal alkynes.[8,10]

In another reactivity paradigm, the salts of transition metals can also act as bifunctional Lewis acids, activating C−C multiple bonds via π-binding or/and generating σ-complexes with heteroatoms, as conventional Lewis acids, such as BF_3, $AlCl_3$, etc., do.[11] Accordingly, the oxophilic character of gold complexes and their activation of oxygen compounds have also been explored. Hence, it is thought that a proper choice of a Lewis acid, which may exhibit a dual role, can lead to the activation of both C−C and C−X multiple bonds in a single transformation,[12,13] and a study on this subject with gold(III) has been recently reported by Jin and Yamamoto.[14] Gevorgyan and co-workers have also observed from a study on a bromoallenyl ketone (C−O double bonds in carbonyl groups can be activated for the addition of a nucleophile) an enhanced oxophilic behavior for gold(III) with respect to the more carbophilic gold(I).[15] Calculations by Straub support this notion of functional group discrimination and indicate that Au(III) exhibits a thermodynamic preference for aldehyde over alkyne coordination. However, this preference does not preclude Au(III)-catalyzed transformations that proceed through alkyne-activation pathways.[16] Nolan, Maseras, and co-workers have recently reported an experimental and computational study on the Au(I)-catalyzed formation of α,β-unsaturated carbonyl compounds from propargylic acetates in the presence of water, and their results suggest a preferred catalytic cycle featuring a transfer of the OH moiety bound to the gold center to the triple bond to form a gold allenolate.[17] There are other recent examples in the literature on the activation of oxygen compounds by gold(I), most of them dealing with carbonyl compounds, where the catalyst acts as a Lewis acid and as a result promotes the inter- or intramolecular nucleophilic attack.[18] Epoxides, indeed masked carbonyl precursors, have also been exposed to gold catalysis, and as Hashmi and Sinha[19] and, independently, Liang and co-workers[20] have reported, α- and β-alkynyl epoxides can undergo ring enlargement to furans in the presence of gold salts.[21]

SCHEME 1. Rearrangement of Acyloxypropargyl Oxiranes to Acyloxydivinyl Ketones Reported by Pale et al.[22]

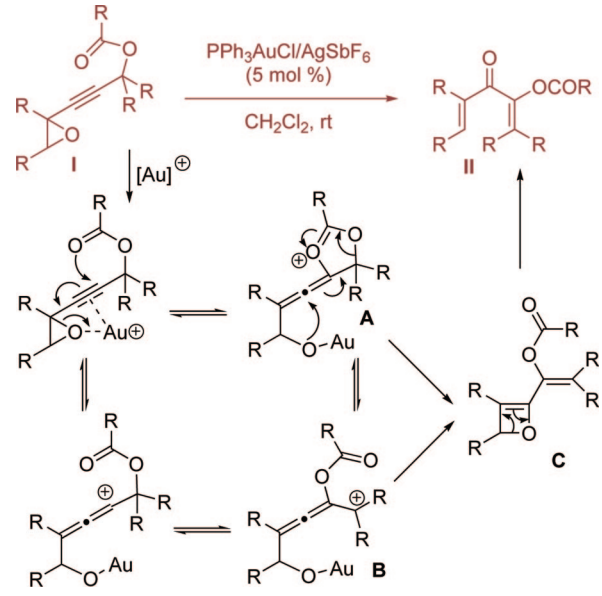

Expanding on this line, Pale et al.[22] have reported a novel rearrangement of (3-acyloxyprop-1-ynyl)oxiranes **I** (Scheme 1) to functionalized divinyl ketones **II** under gold(I) catalysis. The reaction is compatible with a wide selection of substrates and occurs under mild conditions in moderate to good yields. Besides its obvious synthetic applications, this process is intriguing from a mechanistic point of view, since at least three different reaction pathways can be postulated depending on which group is activated by the catalyst.

On the basis of the moderate oxophilic character of Au(I), Pale et al. propose a double activation of the acetylene and the

(4) Marco-Contelles, J.; Soriano, E. *Chem.—Eur. J.* **2007**, *13*, 1350.
(5) Marion, N.; Nolan, S. P. *Angew. Chem., Int. Ed.* **2007**, *46*, 2750.
(6) Correa, A.; Marion, N.; Fensterbank, L.; Malacria, M.; Nolan, S. P.; Cavallo, L. *Angew. Chem., Int. Ed.* **2008**, *47*, 718.
(7) (a) Johansson, M. J.; Gorin, D. J.; Staben, S. T.; Toste, F. D. *J. Am. Chem. Soc.* **2005**, *127*, 18002. (b) Gorin, D. J.; Dubé, P.; Toste, F. D. *J. Am. Chem. Soc.* **2006**, *128*, 14480.
(8) Soriano, E.; Marco-Contelles, J. *Chem.—Eur. J.* **2008**, *14*, 6771.
(9) (a) Marion, N.; Díez-González, S.; de Frémont, P.; Noble, A. R.; Nolan, S. P. *Angew. Chem., Int. Ed.* **2006**, *45*, 3647. (b) Zhang, L. *J. Am. Chem. Soc.* **2005**, *127*, 16804. (c) Zhang, L.; Wang, S. *J. Am. Chem. Soc.* **2006**, *128*, 1442. (d) Wang, S.; Zhang, L. *Org. Lett.* **2006**, *8*, 4585. (e) Oh, C. H.; Kim, A.; Park, W.; Park, D. I.; Kim, N. *Synlett* **2006**, 2781; (f) Buzas, A.; Gagosz, F. *J. Am. Chem. Soc.* **2006**, *128*, 12614. (g) Buzas, A.; Istrate, F.; Gagosz, F. *Org. Lett.* **2006**, *8*, 1957. (h) Wang, S.; Zhang, L. *J. Am. Chem. Soc.* **2006**, *128*, 14274. (i) Zhao, J.; Hughes, C. O.; Toste, F. D. *J. Am. Chem. Soc.* **2006**, *128*, 7436. (j) Lemière, G.; Gandon, V.; Cariou, K.; Fukuyama, T.; Dhimane, A. L.; Fensterbank, L.; Malacria, M. *Org. Lett.* **2007**, *9*, 2207. (k) Wang, S.; Zhang, L. *J. Am. Chem. Soc.* **2006**, *128*, 8414. (l) Yeom, H. S.; Yoon, S. J.; Shin, S. *Tetrahedron Lett.* **2007**, *48*, 4817. (m) Barluenga, J.; Riesgo, L.; Vicente, R.; López, L. A.; Tomás, M. *J. Am. Chem. Soc.* **2007**, *129*, 7772.
(10) (a) Mainetti, E.; Mouries, V.; Fensterbank, L.; Malacria, M.; Marco-Contelles, J. *Angew. Chem., Int. Ed.* **2002**, *41*, 2132. (b) Miki, K.; Ohe, K.; Uemura, S. *J. Org. Chem.* **2003**, *68*, 8505. (c) Anjum, S.; Marco-Contelles, J. *Tetrahedron* **2005**, *61*, 4793. (d) Fürstner, A.; Hannen, P. *Chem.—Eur. J.* **2006**, *12*, 3006. (e) Marco-Contelles, J.; Arroyo, N.; Anjum, S.; Mainetti, E.; Marion, N.; Cariou, K.; Lemière, G.; Mouries, V.; Fensterbank, L.; Malacria, M. *Eur. J. Org. Chem.* **2006**, 4618. (f) Moreau, X.; Goddard, J. P.; Bernard, M.; Lemière, G.; López-Romero, J. M.; Mainetti, E.; Marion, N.; Mouriès, V.; Thorimbert, S.; Fensterbank, L.; Malacria, M. *Adv. Synth. Catal.* **2008**, *350*, 43.
(11) Kobayashi, S.; Manabe, K. *Acc. Chem. Res.* **2002**, *35*, 209.
(12) Yamamoto, Y. *J. Org. Chem.* **2007**, *72*, 7817.
(13) (a) Takahashi, K.; Yamamoto, Y. *J. Am. Chem. Soc.* **2002**, *124*, 764. (b) Nakamura, I.; Bajracharya, G. B.; Mizushima, Y.; Yamamoto, Y. *Angew. Chem., Int. Ed.* **2002**, *41*, 4328.
(14) Jin, T.; Yamamoto, Y. *Org. Lett.* **2008**, *10*, 3137.
(15) Xia, Y.; Dudnik, A. S.; Gevorgyan, V.; Li, Y. *J. Am. Chem. Soc.* **2008**, *130*, 6940.
(16) Straub, B. F. *Chem. Commun.* **2004**, 1726.
(17) Marion, N.; Carlqvist, P.; Gealageas, R.; de Frémont, P.; Maseras, F.; Nolan, S. P. *Chem.—Eur. J.* **2007**, *13*, 6437.
(18) (a) Lin, C. C.; Teng, T.-M.; Odedra, A.; Liu, R.-S. *J. Am. Chem. Soc.* **2007**, *129*, 3798. (b) Dudnik, A. S.; Sromek, A. W.; Rubina, M.; Kim, J. T.; Kel'in, A. V.; Gevorgyan, V. *J. Am. Chem. Soc.* **2008**, *130*, 1440.
(19) Hashmi, A. S. K.; Sinha, P. *Adv. Synth. Catal.* **2004**, *346*, 432.
(20) (a) Shu, X.-Z.; Liu, X.-Y.; Xiao, H.-Q.; Ji, K.-G.; Guo, L.-N.; Qi, C.-Z.; Liang, Y.-M. *Adv. Synth. Catal.* **2007**, *349*, 2493. (b) For enlargement β-epoxy alkynes to pyranones, see: Shu, X.-Z.; Liu, X.-Y.; Ji, K.-G.; Xiao, H.-Q.; Liang, Y.-M. *Chem.—Eur. J.* **2008**, *14*, 5282.
(21) For a related Pt-catalyzed tandem epoxide fragmentation/pentannulation of propargylic esters, see: Pujanauski, B. G.; Bhanu Prasad, B. A.; Sarpong, R. *J. Am. Chem. Soc.* **2006**, *128*, 6786.
(22) Cordonnier, M. C.; Blanc, A.; Pale, P. *Org. Lett.* **2008**, *10*, 1569.

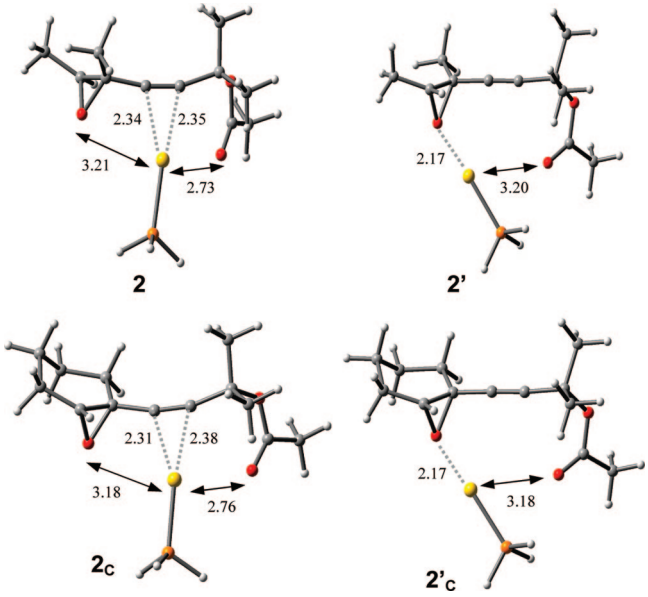

FIGURE 1. Optimized structures of the plausible reactant complexes where gold is coordinated to the alkyne (**2** and $\mathbf{2_C}$) or to the epoxide moiety (**2′** and $\mathbf{2_C}'$). Distances to the catalyst are shown in Å.

oxirane oxygen. This sort of activation would then lead to the induced rearrangement through the formation of the allenic intermediates (**A**, **B**, Scheme 1), which are subsequently attacked by the gold alkoxide. The 2*H*-oxete **C** thus formed is the key intermediate that would afford the final divinyl ketone motif via electrocyclic ring opening. However, two other mechanisms can be invoked for the **I**−**II** transformation where gold behaves in a more conventional way. In these two alternatives, gold acts as a π-electrophilic catalyst by promoting a 1,2- or 1,3-rearrangement of the propargylic ester through the nucleophilic attack of the ester oxygen to the acetylene−gold π-complex (Scheme 6).

Results and Discussion

We therefore decided to study these three mechanisms for the gold-catalyzed transformation of the model system **1** (Scheme 6), where all the R's are methyl groups and triphenylphosphine has been replaced by PH_3 in order to reduce the computational burden.

In addition, we have performed calculations on the cyclic analogue (denoted hereafter with "**C**" subscript) $\mathbf{1_C}$, which was one of the substrates successfully submitted to the catalysis conditions described by Pale.[22] A comparison between **1** and $\mathbf{1_C}$ should provide further mechanistic insights by assessing the effect of the precursor structure on the reaction energy profile.

We begin our study with the gold coordination step. In line with the discussion in the Introduction about the modest oxophilic character of gold being the source of interesting reactivity, we find that coordination of the gold complex to **1** is only (for the open system) 0.4 kcal/mol more stable at the alkyne (**2**) than at the oxirane oxygen (**2′**) (see Figure 1). This unexpected result is further amplified if electronic energies instead of free energy values are compared, since the balance would then be shifted toward coordination to the epoxide by 3.2 kcal/mol (see Table 1). Conversely, for the cyclic analogue $\mathbf{1_C}$, coordination to the oxirane oxygen yields a complex $\mathbf{2_C}'$ 6.0 kcal/mol more stable (4.0 kcal/mol in terms of electronic energy) than coordination to the alkyne moiety $\mathbf{2_C}$. Hence, the different stabilization of the reactant gold complex between both systems can be ascribed to entropic effects. Gold's appetite for oxygen in these molecules can be explained through electrostatic interactions between the positively charged gold complex and the electron-rich oxygens on the oxirane and the carboxylate. The most favored conformations for both **2** and **2′** are rather crowded, with gold, acetate, and the oxirane oxygen on the same side of the alkyne, thus minimizing the charge separation and placing oxygens on the latter functional groups at interacting distances from gold: 2.73 and 3.21 Å in **2** and 3.20 and 2.17 Å (bonding distance) in **2′** for the carboxylate and the epoxide, respectively. The energy differences with respect to their less crowded *anti* counterparts where this interaction/alignment with the acetate is not available are about 6 kcal/mol. When gold is coordinated to the epoxide (**2′**), the electrostatic interaction of gold with the oxygens is maximized, resulting in a stabilization that is compensated with the larger conformational flexibility of the alkyne complex in **2**. The free energy barrier for the transformation between **2** and **2′** is not trivial, 10.4 kcal/mol.

TABLE 1. Relative Free and Activation Energies (in kcal/mol, 298.15 K) Computed at the B3LYP/6-31G(d)-LANL2DZ Level for the Au^IPH_3-Catalyzed Rearrangement of 1[a]

a			*b*			*c*		
	ΔG	ΔG‡		ΔG	ΔG‡		ΔG	ΔG‡
2	0.0							
TS2-2'	10.4	10.4						
2'	0.4							
TS2-3	6.3	6.3	**TS2-11**	9.5	9.5	**TS2-15**	12.1	12.1
3	-8.4		**11**	-7.1		**15**	0.6	
TS3-4	-5.4	3.0	**TS11-12**	9.3	16.5	**TS15-16**	**29.0**	**28.4**
4	-6.3		**12**	4.0		**16**	0.6	
TS4-4'	1.0	7.3	**TS12-13**	22.3	18.4	**TS16-17**	15.5	14.9
4'	-0.5		**13**	21.1		**17**	-15.2	
TS4'-4''	11.4	11.9	**TS13-14**	**25.2**	**4.2**	**TS17-14**	-3.9	11.2
4''	-0.9		**14**	-18.8				
TS4''-5	**11.7**	**12.6**	**TS14-18**	-7.7	11.1			
5	4.3							
TS5-6	8.0	3.8						
6	-30.0							
TS6-7_in	-6.5	23.5						
TS6-7_out	-7.0	23.0						
7_in	-10.9							
7_out	-15.2							
TS7-8	-13.4	1.8						
8	-19.9							
TS8-9	-16.8	3.1						
9	-44.0							

[a] The rate-limiting step for each path is highlighted in boldface. In red, we have highlighted the thermodynamic data corresponding to the transition states for the open system where torquoselectivity is found. In this last case, the transition structures and minima denoted with "in" refer to structures where either the terminal methyl groups are rotating inward or the newly formed alkenes have a Z geometry.

For the discussion of the mechanistic alternatives (Scheme 6), we have chosen **2** as the starting point, since gold activation of the alkyne is needed for two of the three mechanisms, one of them the lowest in energy.

The first mechanism considered (see Scheme 2) involves a reaction path characterized by the nucleophilic attack of the oxirane to an allene intermediate that originates from the 1,3-ester migration.

From the gold coordinated alkyne **2**, a low barrier (6.3 kcal/mol) *anti*-1,3-acetate migration yields allene **4**, through a fleeting intermediate cyclic structure **3**. From here, nucleophilic attack of the oxirane to the cumulene carbon and ring opening are needed for the conversion of **4** into **6**, the 2,5-dihydrofuran

SCHEME 2. Mechanism for the Transformation of 1 into 10, Starting from a 1,3-Ester Migration[a]

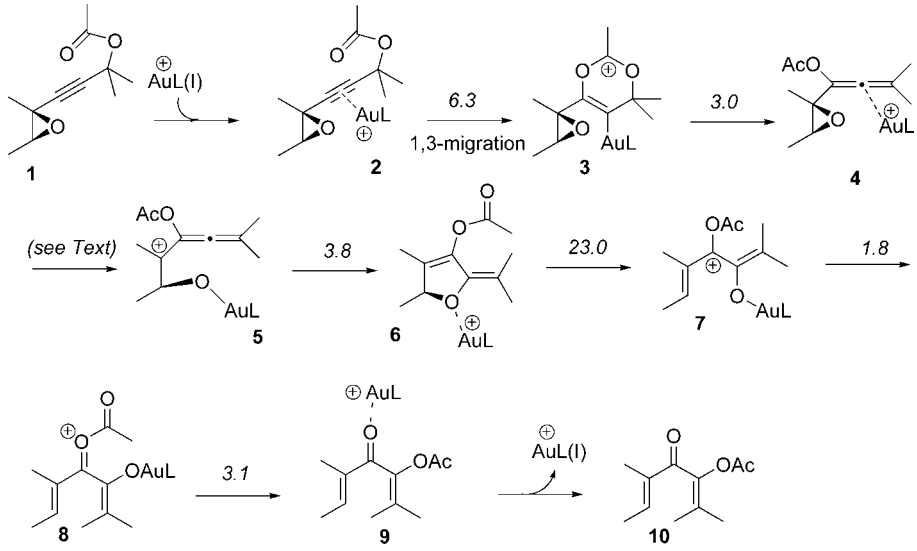

[a] Activation free energies for the depicted processes are noted in kcal/mol over the corresponding arrow (L = PH_3).

SCHEME 3. Detailed Description of the Transformation of 4 into 6

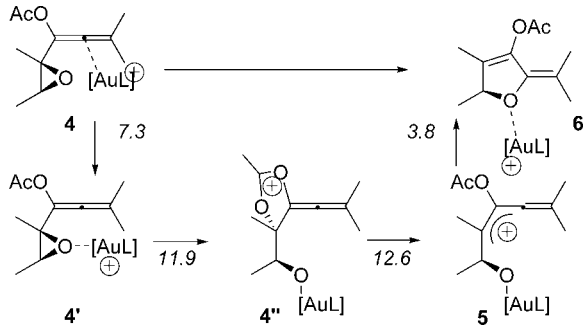

intermediate key in this rearrangement. Two mechanisms can be drawn for this transformation (Scheme 3): a concerted path, where the new C−O bond is formed at the same time the internal C−O bond of the oxirane is breaking, and a stepwise mechanism, where gold activation of the oxirane facilitates its opening, leading to a gold alkoxide that yields **6** after nucleophilic attack to the cumulene carbon. To help discern between these two alternatives, we decided to map the potential energy surface along the two reaction coordinates: the cumulene carbon−oxygen distance and the internal carbon−oxygen distance on the oxirane (Figure 2). Relative SCF energies were employed to build this three-dimensional surface where anchimeric assistance is not considered. The surface is very flat around the transition state corresponding to the oxirane ring opening (the rate-limiting step for this transformation), and a stationary point cannot be properly located in this area. Once this first bond is broken, we find $\mathbf{TS_{5-6}}$ along the reaction coordinate corresponding to the five-membered-ring closure. According to this representation, a concerted path for the **4** to **6** transformation is not feasible, with high energy values and no stationary points in the region of intermediate C−O bond distances.

Gold switches coordination between the allene and the oxirane oxygen, with a barrier of 7.3 kcal/mol. The oxirane ring opening in the resultant **4′** is then assisted by the anchimeric effect of the neighboring acetate, forming the gold allenolate **4″** via an intramolecular S_N2 reaction, with a barrier of 11.9 kcal/mol. The ensuing ring opening of the heterocycle by C−O cleavage leads to **5** and leaves the reactive groups poised to undergo the alkoxycyclization to **6**. For the acyclic system, the formation of the intermediate **5** is the rate-limiting step of this mechanism (see Figure 5). The allenolate **5** readily rearranges, through an early $\mathbf{TS_{5-6}}$ (C−O distance, 2.32 Å) with an energy barrier of 3.8 kcal/mol, to the cyclic product **6**.

The opening of the dihydrofuran ring in **6** is the key step in this rearrangement and the highest reaction barrier in this branch of the mechanistic manifold, due to the stability of the conjugated diene (∼30 kcal/mol lower in energy than the reactant complex). Gold activation of the ring oxygen is essential to stabilize the negative charge buildup at this center on $\mathbf{TS_{6-7}}$. In the open model system, this ring opening can proceed through two different transition states, depending on whether the terminal methyl group rotates inward or outward with respect to the ring backbone. The process, however, is favored for the formation of the *E* with respect to the *Z* alkene from kinetic (by 0.5 kcal/mol) and thermodynamic (by 4.3 kcal/mol) standpoints (see Table 1).

The transformation of **7** into **8** is then achieved through a low-barrier σ-bond rotation, which is followed by a migration of the acetyl group promoted by nucleophilic attack of the gold enolate that leads to the final product **10** after gold is removed.

A second mechanism for this transformation can be proposed, in which gold mediation occurs via carbenoid chemistry through an initial 1,2-rearrangement (see Scheme 4). This path is initiated with a 1,2-ester rearrangement on the activated alkyne and the concomitant formation of a σ C−Au bond to furnish **11**. The activation barrier for this process is 3.2 kcal/mol higher than for the alternate 1,3-migration (see Scheme 2). We found a preference for *syn*-addition of the acetate to provide the vinyl gold intermediate **11** with *Z* geometry. The migration is then completed with the formation of the gold carbenoid **12**. After this, the oxirane undergoes an unusual ring expansion in two steps. The first one involves the attack of one of the oxygen lone pairs to the carbene carbon atom, thus forming the highly unstable oxonium ion **13**. The second step completes the ring expansion of the fleeting intermediate **13** affording 2*H*-oxete **14**. The electrocyclic ring opening of **14**, the rate-limiting step

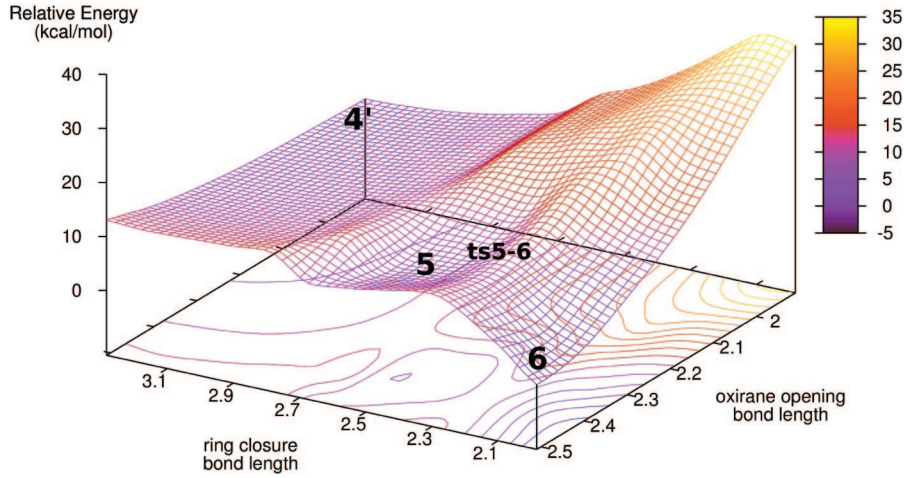

FIGURE 2. Potential energy surface along the main reaction coordinates involved in the transformation of **4′** (gold coordination to the oxirane in **4**) into **6**, computed at the B3LYP/6-31G(d)-LanL2DZ level.

SCHEME 4. Mechanism for the Transformation of 1 into 10, Starting from a 1,2-Ester Migration That Leads to Carbenoid Intermediate 12[a]

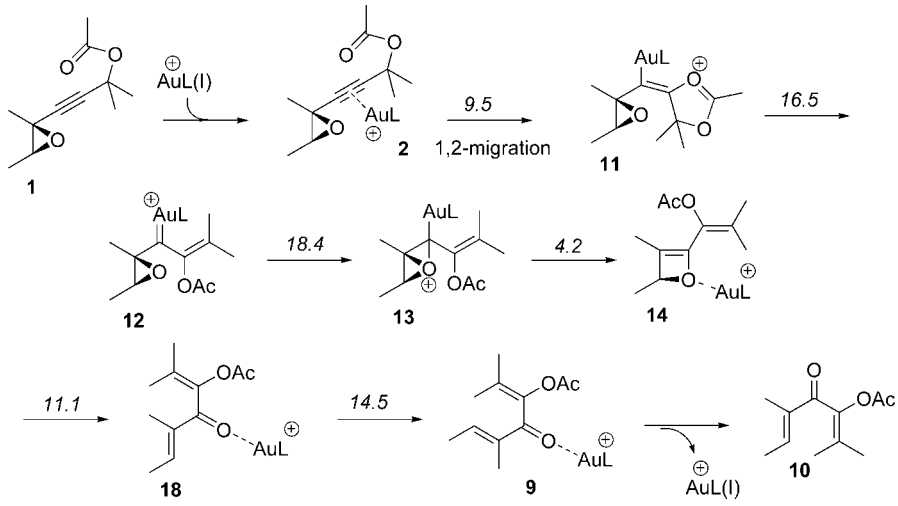

[a] Activation free energies for the depicted processes are noted in kcal/mol over the corresponding arrow (L = PH_3).

in this path, leads to the gold-complexed acetoxydivinyl ketone **18** that evolves to the product **10** upon the elimination of the catalyst.

The singularity of this last two-step ring expansion was the subject of further investigation. A thorough two-dimensional scan of the potential energy surface around $\mathbf{TS_{12-13}}$−**13**−$\mathbf{TS_{13-14}}$ showed a high energy plateau in the area associated with the concerted ring expansion, ruling out the possibility of the more common ring expansion via σ-bond migration (see Figure 3).

A third possibility for this transformation deals with the pathway proposed by Pale and co-workers, through a plausible oxirane activation that steers the mechanism toward the formation of an allene intermediate (see Scheme 5).

This path proceeds by initial activation of the epoxide by the catalyst. The complexation to the oxygen allows the opening of the oxirane ring, which induces the simultaneous trapping of the electrophilic distal allenic carbon by the ester group to afford **15** along a *syn*-S_N2' trajectory. The barrier for this transformation (12.1 kcal/mol) is the highest among the three initial steps considered. The allene intermediate **15** undergoes then an alkoxycyclization[23] to form the 2*H*-oxete **16** in the less favored step along the profile, with a 28.4 kcal/mol barrier. The subsequent 1,2-acyl rearrangement and gold coordination to the oxete oxygen leads to **14**, the structure where this mechanism converges with the second reaction path described. The final acyloxydivinyl ketone is then formed via a facile electrocyclic ring opening of **14**. For the open system, there are two possible directions of conrotation for the step, but our calculations suggest that the reaction enforces a tight stereo(torquo)control[24] that exclusively would lead to the *E* olefin (difference between barriers of 7.4 kcal/mol).

At this point, we set out to validate the methodology used around two key issues that often raise concerns in these kind of systems: the size of the basis set and the neglect of solvent effects.

For the first, we compare (Figure S1, Supporting Information) the free energy profiles for the three paths available for the rearrangement of **1** when computed using B3LYP/6-31G(d),

(23) Allene hydrocarbons are not susceptible to nucleophilic addition reactions unless the allene is activated with an electron-withdrawing group. For unactivated allenes, good nucleophiles such as phenoxides are required; see: Gaertner, R. *J. Am. Chem. Soc.* **1951**, *73*, 4400.

(24) (a) Rondan, N. G.; Houk, K. N. *J. Am. Chem. Soc.* **1985**, *107*, 2099. (b) Dolbier, W. R.; Koroniak, H.; Houk, K. N.; Sheu, C. *Acc. Chem. Res.* **1996**, *29*, 471.

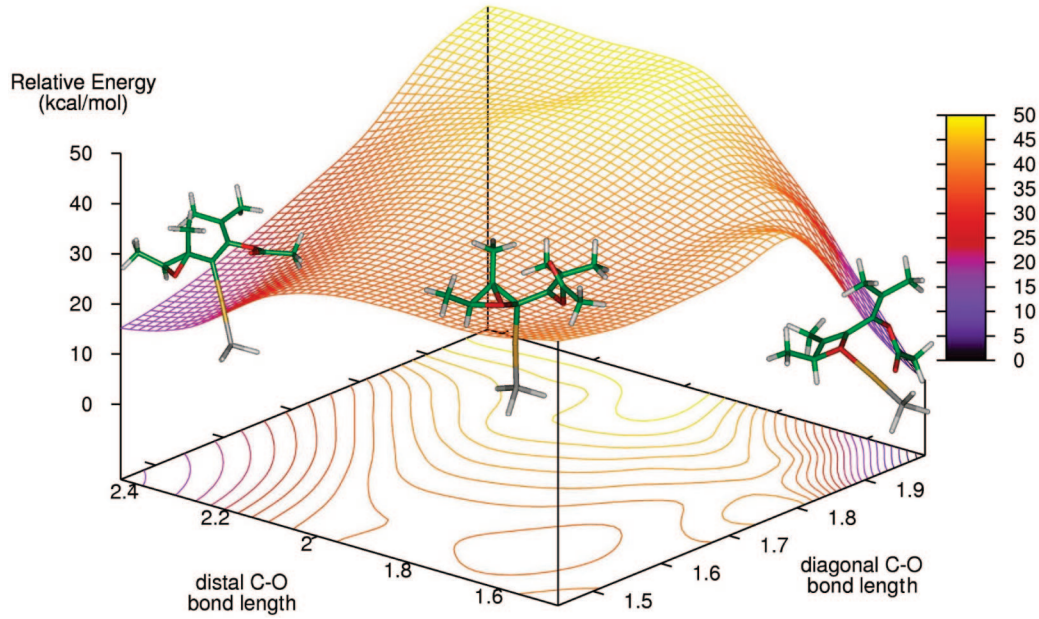

FIGURE 3. Potential energy surface for the **12**−**13**−**14** transformation computed at the B3LYP/6-31G(d)-LanL2DZ level (relative SCF energies). The high energy plateau associated with the concerted ring expansion rules out the possibility of the more common ring expansion via σ-bond migration. The geometries associated with the three minima (**12**, **13**, and **14**) are displayed over the stepwise path.

SCHEME 5. Mechanism for the Transformation of 1 into 10, through Oxirane Activation and the Formation of an Allene[a]

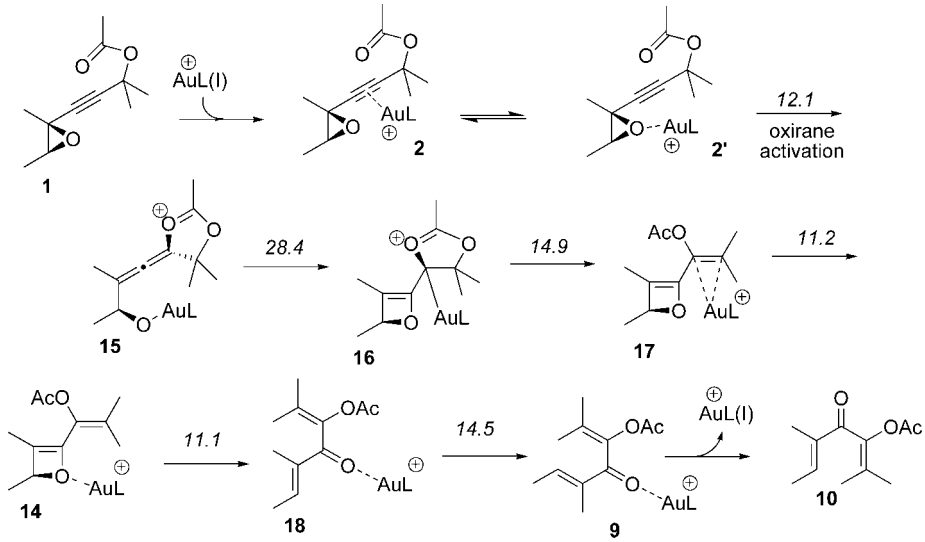

[a] Activation free energies for the depicted processes are noted in kcal/mol over the corresponding arrow (L = PH_3).

LANL2DZ as described in the Methods and the corresponding profiles after a single-point energy correction using a triple-ζ plus polarization basis set for light and heavy atoms with the 6-311G(d,p) and LANL2TZ(f) sets.[25] From the plot, we conclude that the energy refinement does not affect the preference for one mechanism over another and only slightly changes the barriers within each profile.

The problem of solvation is more complex. In our experience, even with cationic processes as those described for the rearrangement of **1**, the simulation of the solvent environment using a continuum method (the only technique feasible for this system) does not alter much the mechanism of Au(I)-catalyzed rearrangements,[26] or pentadienyl cation electrocyclizations,[27] specially if the reaction takes place in a solvent with a small dielectric constant such as CH_2Cl_2. However, since there is ample evidence of organic transformations where the presence of solvent dramatically affects the outcome of the reaction, we decided to correct the free energies discussed up to this moment with a solvation term. Solvation free energies have been calculated on the gas-phase optimized geometries, using the PCM method, with UAKS radii and the dielectric constant of dichloromethane. The resultant reaction profiles in solution (shown in Figure S2, Supporting Information, together with the gas-phase profiles for each of the three paths available for the

(25) Roy, L. E.; Hay, P. J.; Martin, R. L. *J. Chem. Theory Comput.* **2008**, *4*, 1029.

(26) Nieto Faza, O.; Silva López, C.; Álvarez, R.; de Lera, A. R. *J. Am. Chem. Soc.* **2006**, *128*, 2434.

(27) Nieto Faza, O.; Silva López, C.; Álvarez, R.; de Lera, A. R. *Chem.—Eur. J.* **2004**, *10*, 4324.

TABLE 2. Relative Free and Activation Energies (in kcal/mol, 298.15 K) Computed at the B3LYP/6-311G(d,p)-LANL2TZ(f) Level for the Au^{I}PPh$_3$-Catalyzed Rearrangement of 1[a]

a			b			c		
	ΔG	ΔG‡		ΔG	ΔG‡		ΔG	ΔG‡
$\mathbf{2_{Ph}}$	0.0							
TS2-2'	10.8	10.8						
$\mathbf{2_{Ph}}$ **'**	-1.1							
TS2-3	7.7	7.7	**TS2-11**	12.3	12.3	**TS2-15**	14.1	15.1
$\mathbf{3_{Ph}}$	-0.4		$\mathbf{11_{Ph}}$	-0.6		$\mathbf{15_{Ph}}$	4.6	
TS3-4	1.2	1.7	**TS11-12**	14.0	14.5	**TS15-16**	**32.2**	**27.7**
$\mathbf{4_{Ph}}$	-5.4		$\mathbf{12_{Ph}}$	7.0		$\mathbf{16_{Ph}}$	9.1	
TS4-4'	2.3	7.6	**TS12-13**	27.3	20.3	**TS16-17**	19.8	10.7
$\mathbf{4_{Ph}}$ **'**	-1.6		$\mathbf{13_{Ph}}$	25.3		$\mathbf{17_{Ph}}$	-13.0	
TS4'-4"	11.1	12.7	**ts13-14**	**28.7**	**3.5**	**TS17-14**	-3.0	10.1
$\mathbf{4_{Ph}}$ **"**	2.6		$\mathbf{14_{Ph}}$	-18.9				
TS4"-5	**15.0**	**12.3**	**TS14-18**	-7.5	11.4			
$\mathbf{5_{Ph}}$	3.3		$\mathbf{18_{Ph}}$	-43.8				
TS5-6	7.0	3.6						
$\mathbf{6_{Ph}}$	-32.4							
TS6-7_in	-6.5	25.9						
TS6-7_out	-8.5	23.9						
$\mathbf{7_{Ph}}$**_in**	-10.6							
$\mathbf{7_{Ph}}$**_out**	-16.6							
TS7-8	-13.4	3.2						
$\mathbf{8_{Ph}}$	-19.9							
TS8-9	-18.4	1.5						
$\mathbf{9_{Ph}}$	-46.5							

[a] The rate-limiting step for each path is highlighted in boldface. In red, we have highlighted the thermodynamic data corresponding to the transition states for the open system where torquoselectivity is found. In this last case, the transition structures and minima denoted with "in" refer to structures where either the terminal methyl groups are rotating inward or the newly formed alkenes have a *Z* geometry.

evolution of **1**) are almost superimposable, so the effect of solvation on the barriers within each path and in the competition between mechanisms is negligible.

Even if in our previous experience with similar Au(I)-catalyzed systems the nature of the ligands on the metal center does not significantly affect the calculated barriers,[26] the extreme simplification introduced when modeling through hydrogen atoms the phenyl groups on the phosphine used in the experiment, might lead to spurious results in a system as complex and crowded as this. To assuage these concerns and evaluate whether our previous observations are an isolated phenomenon or can be generalized to other systems, we have reoptimized all the stationary points in our profiles explicitly including the PPh_3 ligand (structures denoted with the "**Ph**" subscript in Table 2).

The introduction of the phenyl groups on the phosphorus atom does not seem to introduce a significant electronic distortion of the reacting backbone, as the steps where the barriers most differ from those calculated with PH_3 are those where the volume of the ligand leads to large steric interactions. Examples of this are $\mathbf{TS_{16-17}}$ (the barrier goes from 14.9 kcal/mol with PH_3 to 10.7 kcal/mol with PPh_3) where gold changes its coordination from a σ-bond to the proximal carbon of the alkene to a longer π-bond to this alkene, further away from the crowded oxete or the clearer differentiation between the *in* and *out* paths in $\mathbf{TS_{6-7}}$ when PPh_3 is the ligand used.

As can be seen in Table 2, the three profiles with PPh_3 lie in general about 3 kcal/mol below those calculated with PH_3 but, as happened with the change of base or the introduction of solvent effects, the reactivity we have described and discussed is not altered. The same three mechanisms through the same set of steps are available for the **1**−**10** transformation; mechanism a, starting from a 1,3-ester migration, is still the preferred reaction path, and the rate-limiting steps for each mechanism are still $\mathbf{TS_{4''-5}}$, $\mathbf{TS_{13-14}}$, and $\mathbf{TS_{15-16}}$. The ordering of the activation free energies for the global mechanisms is a < b < c in both cases ($\mathbf{TS_{4''-5}} < \mathbf{TS_{13-14}} < \mathbf{TS_{15-16}}$), and the energetic preferences for a over b and for b over c are very similar: 13.8 (PH_3)/13.5 (PPh_3) kcal/mol for the gap between mechanisms a and b, and 3.5 (PH_3)/3.8 (PPh_3) kcal/mol for the gap between mechanisms b and c.

Thus, we can safely assume that the use of PH_3 as a model of the much larger ligand PPh_3 is not introducing undesirable effects in our interpretation of the reactivity discussed, and we can use this simplification in our treatment of the more complex cyclic system $\mathbf{1_C}$.

Thus, we have described, with confidence in the approximations introduced, three possible reaction paths for the rearrangement that leads from **1** to **10**. These three mechanisms, depicted together in Scheme 6 and Figure 4, combine a wide repertoire of known Au(I)-catalyzed enyne and alkynyloxirane reactivity with the effect of an intramolecular nucleophile and are characterized by the following: (a) the nucleophilic attack of the oxirane to an allene intermediate that originates from 1,3-ester migration; (b) gold mediation occurring via carbenoid chemistry through an initial 1,2-rearrangement; (c) the pathway proposed by Pale and co-workers, proceeding through a plausible oxirane activation. The availability of at least three different reasonable reaction paths for this rearrangement, the sheer number of steps involved in the transformation, the intrincate interplay between functional groups, and the dual role of the catalyst in sequentially coordinating insaturations or the oxygen atom showcase the possibilities of Au(I) as a catalyst in generating complexity with selectivity and caution us against straightforward mechanistic assumptions.

The most favorable path by 13.5 kcal/mol is that starting from 1,3-ester migration and proceeding through essentially open structures (a in Scheme 6 and Figure 4) that avoid the costly formation of the intermediate oxete **14**. Despite their being substantially higher in energy and thus noncompetitive (Figure 4), the study of branches b and c provides insight into the catalytic gold manifold and the delicate interplay between the metal center and the different functional groups of the substrate.

As explained above, we also characterized these same three profiles for the rearrangement of the cyclic system $\mathbf{1_C}$ (see Scheme 6). As can be inferred from the data in Tables 1 and 3, the introduction of the ring in $\mathbf{1_C}$ does not have major effects in the preference for the mechanism triggered by 1,3-ester migration over the other two possibilities, in the sequence of steps involved in each of the three paths, or in the rate-limiting steps. The main differences with respect to the acyclic model are found in some transition structures whose associated barriers are noticeably lower thanks to the release of strain involved or the favorable conformation provided by the cyclic tether. Those transition structures in the first mechanism: $\mathbf{TS_{2-3}}$, $\mathbf{TS_{4-4'}}$, $\mathbf{TS_{4''-5}}$, or $\mathbf{TS_{6-7}}$ result in the rearrangement being slightly more favorable for the cyclic system (about 1.5 kcal/mol), except for $\mathbf{TS_{4''-5}}$ which reveals a larger difference (by 8 kcal/mol). The spirocycle framework in $\mathbf{4_C''}$, whose formation is now the rate-limiting step, involves an annular strain that destabilizes the acetal intermediate in relation to the acyclic system (by about 2 kcal/mol). This annular tension is relieved in the transition structure for the acetal opening $\mathbf{TS_{4''-5}}$, which is reached earlier than for the acyclic system (breaking bond C−O = 2.184 vs 2.228 Å, respectively) as a result. Lower barriers for the cyclic system are also found for the 1,2-ester migration ($\mathbf{TS_{2-11}}$) and the formation of the allene ($\mathbf{TS_{2-15}}$) in the other two mecha-

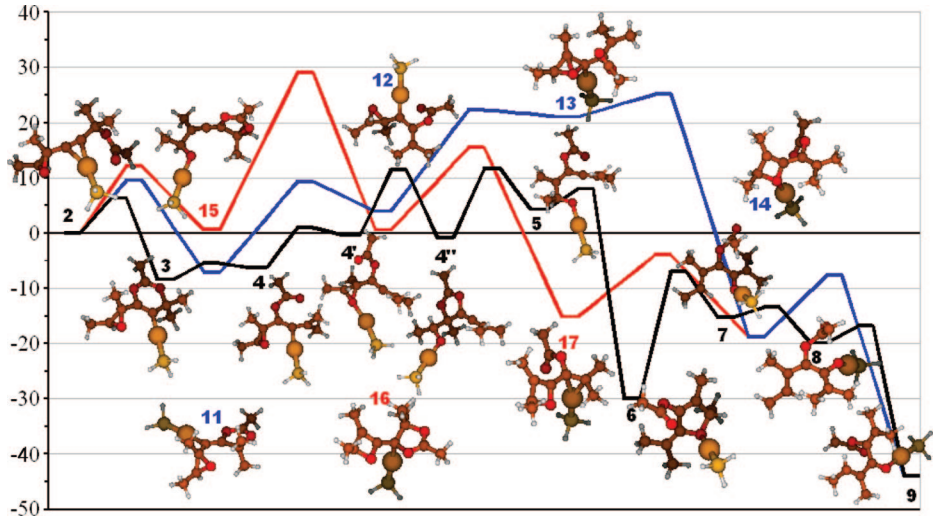

FIGURE 4. Free energy profiles (kcal/mol) for the three mechanisms studied for the rearrangement of **1** to **10**. Color code: black = path a; blue = path b; red = path c.

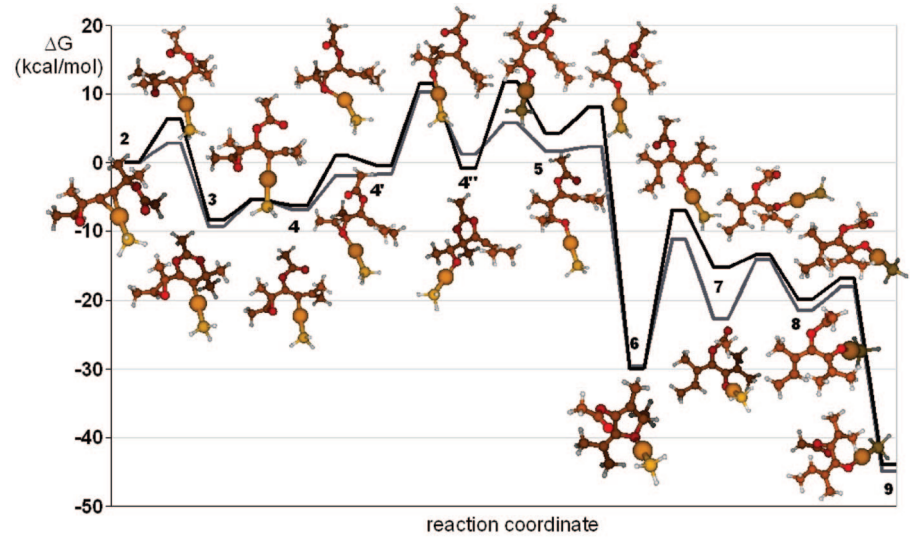

FIGURE 5. Comparison between the free energy profiles for the gold-catalyzed rearrangement of (3-acyloxyprop-1-ynyl)oxiranes **1** (in black) and $\mathbf{1_C}$ (in gray). The cyclized precursor $\mathbf{1_C}$ shows a slightly more favorable profile because of the ring strain release in some steps.

nisms. For the second path the reaction is, however, less favorable for the cyclic system (by 2.6 kcal/mol), due to the extra strain imposed by the additional ring in the high energy intermediate (**13**) leading to the rate-limiting step, $\mathbf{TS_{13-14}}$. Despite a more favorable first step for the cyclic system in the third mechanism, the reaction barrier for the overall mechanism is not altered upon this structural modification.

Figure 5 depicts a comparison of the free energy profiles for the rearrangement of **1** and $\mathbf{1_C}$ along the most favorable mechanism. The relevant free energies for all of the three profiles can be found in Table 1 for the acyclic system and Table 3 for the cyclic model.

Furthermore, the fact that there is a mechanistic alternative that involves oxirane activation, with no intervention of π alkyne-gold complexes, invites us to explore the possibility of catalysis by non-metal Lewis acids, so the analogous BF_3-activated rearrangement of **1** (Scheme 7) was also studied.

The rate-limiting step for this rearrangement of **1** through BF_3-activation and ring opening of the oxirane is of higher energy than its gold-catalyzed counterpart (19.7 vs 11.7 kcal/mol, respectively) but lower in energy than the gold allene pathway starting from acetyl 1,2-migration on **2′**. The nonmetal oxirane activation is also more efficient in terms of the number of steps involved due to a greater degree of concert in the key transformations. In the first step, the oxirane ring opens with assistance of the propargyl ester to yield the allene **15B**. Subsequent nucleophilic attack occurs also in concert (in contrast to the gold-activated variant) with the completion of the acetyl migration to furnish 2*H*-oxete **14B**. Lastly, the electrocyclic ring opening of **14B** produces the final activated divinyl ketone **9B**. This latter step occurs with complete torquoselectivity to yield the *E* olefin. Finally, it should be noted that the uncatalyzed ring opening proceeds with a notably higher energy barrier (19.8 vs 16.4 kcal/mol), which rules it out as an operative event.

Conclusions

We have described three competing paths for the Au(I)-catalyzed rearrangement of acyloxypropargyl oxiranes to acy-

(28) (a) Becke, A. D. *J. Chem. Phys.* **1993**, *98*, 5648. (b) Lee, W.; Yang, R. G.; Parr, R. G. *Phys. Rev. B: Condens. Matter Mater. Phys.* **1988**, *37*, 785.

TABLE 3. Relative Free and Activation Energies (in kcal/mol, 298.15 K) Computed at the B3LYP/6-31G(d)-LANL2DZ Level for the $Au^{I}PH_3$-Catalyzed Rearrangement of 1_C[a]

a			b			c		
	ΔG	ΔG‡		ΔG	ΔG‡		ΔG	ΔG‡
2_C	0.0					$2'_C$	-6.0	
TS_{2-3}	2.8	2.8	TS_{2-11}	7.1	7.1	TS_{2-15}	10.5	10.5
3_C	-9.3		11_C	-8.6		15_C	5.6	
TS_{3-4}	-5.4	3.9	TS_{11-12}	3.2	11.8	TS_{15-16}	**29.3**	**23.7**
4_C	-6.9		12_C	-0.2		16_C	0.5	
$TS_{4-4'}$	-2.0	5.0	TS_{12-13}	25.1	24.3	TS_{16-17}	15.7	15.2
$4_C'$	-1.7		13_C	24.3		17_C	-6.1	
$TS_{4'-4''}$	**10.2**	**12.0**	TS_{13-14}	**27.9**	**3.5**	TS_{17-14}	-2.1	4.1
$4_C''$	1.2		14_C	-12.6				
$TS_{4''-5}$	5.8	4.6	TS_{14-8}	-5.7	6.9			
5_C	1.7							
TS_{5-6}	2.3	0.7						
6_C	-29.7							
TS_{6-7}	-11.2	18.5						
7_C	-22.8							
TS_{7-8}	-14.1	8.7						
8_C	-21.5							
TS_{8-9}	-18.1	3.4						
9_C	-45.0							

[a] The rate-limiting step for each path is highlighted in boldface.

loxydivinyl ketones that evidence the multifaceted character of gold as a catalyst in the synthesis of polyfunctional compounds. The preferred mechanism for this facile synthetic transformation involves a sequence of more than eight steps where the dense functionalization of the substrate's backbone is the key of the reactivity: all the groups act in synergy, and sequential gold coordination to the π-system and the lone pairs of oxygen is needed for the rearrangement.

We have also addressed the effect of the structure and found that the transformation of a cyclized precursor is slightly kinetically favored because of the ring strain released in the rate-limiting step.

The solvent (at least in a SCRF approximation) seems not to have a relevant qualitative contribution to the reactivity in this system, and the profiles are strikingly similar to those obtained in the gas phase. The simplification of PPh_3 with PH_3 in the model system does not introduce relevant modifications beyond those originated in limited steric effects in any of the three models of reactivity, resulting in a significant and safe reduction in the computational costs.

Methods

DFT calculations with the B3LYP hybrid functional[28] have been performed using Gaussian03[29] to locate and characterize the stationary points. The 6-31G(d) basis set has been used for the main group, while the LANL2DZ basis set,[30] in which the innermost electrons are replaced by a relativistic effective core potential (ECP) and the valence electrons are explicitly treated by a double-ζ basis set, has been applied to Au. The optimized geometries were characterized by harmonic analysis, and the nature of the stationary points was determined according to the number of negative eigenvalues of the Hessian matrix. In several doubtful cases, the intrinsic reaction coordinate (IRC)[31a] pathways from the transition structures have been followed by using a second-order integration method[31b] to verify the proper connections with reactants and products. Zero-point vibration energy (ZPVE) and thermal corrections (at 298 K, 1 atm) to the energy have been estimated on the basis of the frequency calculations. The accuracy of this model was evaluated on energy calculations on the previously optimized geometries at the triple-ζ level, using the 6-311G(d,p) and LANL2TZ(f) basis set.[25] Solvation effects were also modeled with the self-consistent reaction field (SCRF) method using the so-called polarizable continuum model (PCM)[32] as implemented in Gaussian03, in

SCHEME 6. Mechanistic Alternatives for the Au(I)-Catalyzed Rearrangement (L = PH_3) of Acyloxypropargyl Oxiranes 1 and 1_C[a]

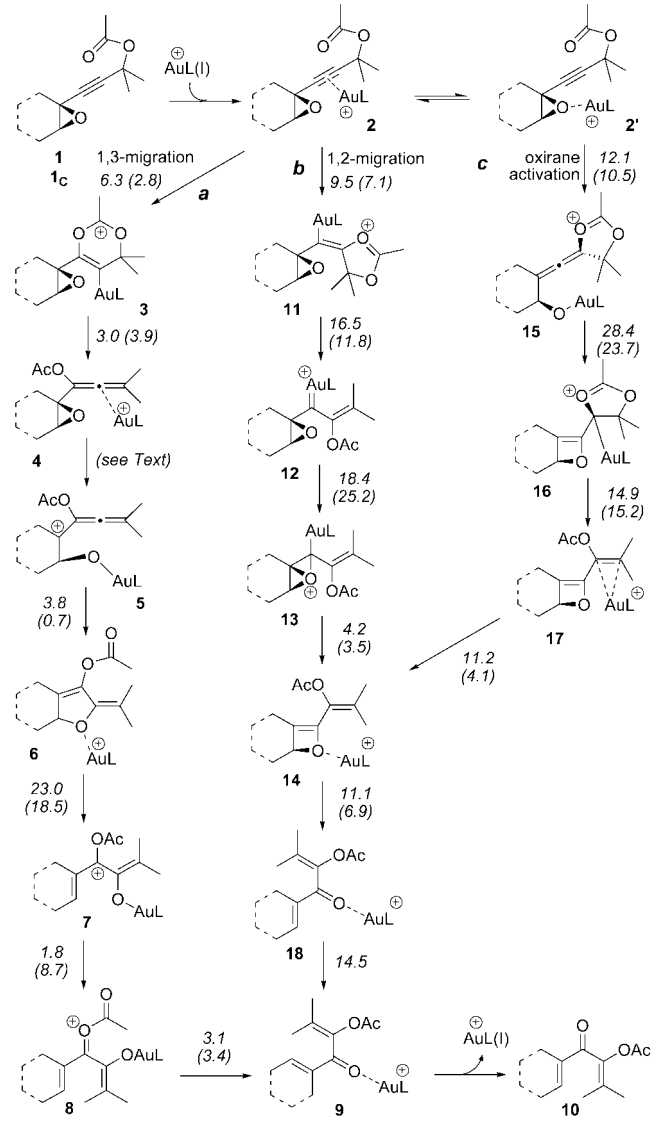

[a] For each step, the free energy of activation (kcal/mol) is indicated in italics (in parentheses for 1_C).

SCHEME 7. BF_3-Catalyzed Rearrangement of 1[a]

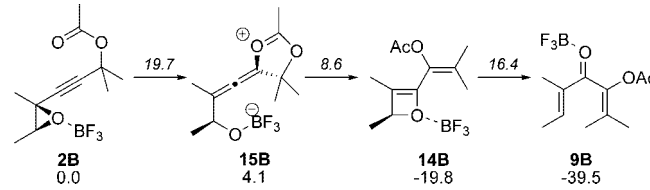

[a] For each step, the free energy of activation (kcal/mol) is indicated in italics.

(29) *Gaussian03*; Gaussian, Inc.: Wallingford, CT, 2004 (see Supporting Information).
(30) Hay, P. J.; Wadt, W. R. *J. Chem. Phys.* **1985**, *82*, 270.
(31) (a) Fukui, K. *Acc. Chem. Res.* **1981**, *14*, 363. (b) González, C.; Schlegel, H. B. *J. Phys. Chem.* **1990**, *94*, 5523.

which the solvent is represented by an infinite dielectric medium characterized by the relative dielectric constant of the bulk. A relative permittivity of 8.93 was assumed to simulate CH_2Cl_2.

Acknowledgment. The authors are grateful to the Xunta de Galicia (Parga Pondal Contract to C.S.L.), the Ramón Areces Foundation (A.G.P. Fellowship), and to the Centro de Supercomputación de Galicia (CESGA) for generous allocation of computing resources.

(32) (a) Tomasi, J.; Persico, M. *Chem. Rev.* **1994**, *94*, 2027. (b) Cossi, M.; Scalmani, G.; Rega, N.; Barone, V. *J. Chem. Phys.* **2002**, *117*, 43.

Supporting Information Available: Additional thermodynamic data, solvated profiles (PCM) for the three paths available to **1**, free energy profiles for the three paths for **1** computed at B3LYP/6-31G* LANL2DZ//B3LYP/6-311G(d,p), LANL2TZ(f), Cartesian coordinates, SCF energies, and the number of imaginary frequencies of all structures. This material is available free of charge via the Internet at http://pubs.acs.org.

JO802516K